# Investigation on Microstructural Behavior of Styroflex/Polyaniline Blends by WAXS

**Siddaramaiah,[1] Fernando G. Souza Jr.,[2] Bluma G. Soares,[2] R. Somashekar[3]**

[1]*Department of Polymer Science and Technology, Sri Jayachamarajendra College of Engineering, Mysore-570006, India*
[2]*Institute of Macromolecules, Federal University of Rio de Janeiro, Centro de Tecnologia, Bl J, Ilha do Fundão, Rio de Janeiro, RJ 21945-970, Brazil*
[3]*Department of Studies in Physics, University of Mysore, Manasagangotri, Mysore-570006, India*

Received 1 July 2010; accepted 20 September 2011
DOI 10.1002/app.35652
Published online 12 December 2011 in Wiley Online Library (wileyonlinelibrary.com).

**ABSTRACT:** Styroflex/polyaniline (STF/PAni) blends were prepared by two routes namely by *in situ* and thermo mechanical processing method with various PAni compositions, namely, 0, 15, 30, and 45 wt %. The influence of volume fraction of PAni in the blends and synthetic routes of the STF/PAni blends on the volume resistivity and microcrystalline parameters have been investigated. The microcrystalline parameters such as the nanocrystal size ($<N>$), lattice disorder ($g$), interplanar distance ($d_{hkl}$), width of the crystallite size distribution, surface weighted crystal size ($D_s$), and crystallite area were evaluated from the wide angle X-ray scattering profiles. The different asymmetric column length distribution functions namely, exponential, reinhold, and lognormal distribution methods were employed to probe the microcrystalline behavior of the STF/PAni blends and the results are compared. © 2011 Wiley Periodicals, Inc. J Appl Polym Sci 124: 5097–5105, 2012

**Key words:** polymer blends; styroflex; polyaniline; conducting blends; WAXS; crystallite size

## INTRODUCTION

Intrinsically conducting polymers (ICPs) are promising materials for broad spectrum of applications. Recently, polymers containing conjugated π-electron systems like polyaniline (PAni), polypyrrole, and polythiophene have been well studied. Among the conducting polymers, PAni has a special interest, within the field of conducting polymers for many reasons such as low monomer cost, simple polymerization methods, a high yield of polymerization product, its high stability toward environmental exposition, redox properties, and special electronic properties, and a wide range of applications. Its wide range of associated electrical, electrochemical, microelectronics, and optical properties[1,2] coupled with good stability, turns PAni into an attractive material for applications such as static films for transparent packaging of electronic components, electromagnetic shielding, rechargeable batteries, light emitting diodes, nonlinear optical devices, sensors for medicine, pharmaceutics, and membranes for the separation of gas mixtures. Further, PAni cannot be processed using simple routine techniques, which are employed in the plastic industry. It is to be noted here that pure PAni has poor mechanical properties.[3]

Techniques based on the dispersion of conducting polymer particles in a matrix comprised of common insulation polymers have been receiving increasing attention and are very attractive due to the possibility of combining the good processability and mechanical performance of the conventional polymer with the electrical and optical properties of PAni. This is due to the fact that there is an increasing demand for polymeric materials whose electrical conductivity can be tailored for a given application and has attractive mechanical properties of the components. The purpose of preparing blends using a conducting polymer along with a high performance commercial polymer is to create a product which widens the applications of conducting polymers.[4]

PAni blends can be prepared by blending PAni with other polymers in solution or in the melt state. Alternatively, aniline can be polymerized chemically or electrochemically in a solution of a matrix polymer. Polymers that have been used to prepare conductive PAni blends include epoxy resin,[4–6] polyethylene,[7] poly(vinyl alcohol),[8,9] chitosan,[10]

*Correspondence to:* Siddaramaiah (Siddaramaiah@yahoo.com).

Contract grant sponsors: Third World Academy of Science (TWAS)-UNESCO Italy, and Conselho Nacional de Desenvolvimento Cienticoe Tecnologico (CNPq), Brasil.

thermoplastic polyurethane,[11] nylon 6,[12] cellulose triacetate,[13] styrene butadiene styrene triblock polymer,[14] ethylene vinyl acetate,[15] and polyacrylonitrile.[16]

Many researchers have characterized PAni composites/blends using wide-angle X-ray scattering (WAXS) and other analytical techniques.[13–19] For the commercial exploitation of conducting polymer blends, insight into their structure-property relationship is very important.

Styroflex (STF), is a special type of styrene-butadiene block copolymer, which has around 70 wt % styrene and possesses mechanical properties very much similar to thermoplastic-elastomer materials (high elongation and elastic properties). The selection of the STF has been made based on its exceptional qualities such as good flexibility, abrasion resistance, smooth surface, easy processability, and its compatibility with different kinds of additives.

This study constitutes an attempt to interpret the observed electrical properties of STF/PAni blends with microstructural parameters, which were evaluated from X-ray profiles by using three different models such as exponential, lognormal, and reinhold asymmetric column length distribution functions. In this research work, STF/PAni blends were prepared by two routes namely *in situ* polymerization and thermo mechanical processing methods. The effects of PAni content and synthetic routes of blending on microcrystalline behavior of the STF/PAni.DBSA have been investigated. The main interest here is producing a soft and reusable material for applications as pressure sensitive, antistatic, or as dielectric materials.

## EXPERIMENTAL

### Materials

Aniline, ammonium persulfate (APS) and other solvents were obtained from M/s. Vetec LTDA, Brasil. Dodecylbenzenesulfonic acid (DBSA) was purchased from Solquim LTDA, Brasil. STF (2G66) containing around 70 wt % of styrene and $M_w = 120{,}000$ g/mol was kindly supplied by M/s. BASF, Brasil.

### Synthesis of PAni.DBSA

PAni doped with DBSA (PAni.DBSA) was synthesized through emulsion polymerization in toluene. In a typical procedure, 4.7 mL (0.051 mol) of aniline and 16.7 g (0.051 mol) of DBSA were dissolved in 250 mL of toluene with constant stirring. The reaction mixture was kept at 0°C and an aqueous solution containing 11.36 g (0.051 mol) of APS in 40 mL of water was slowly added over a period of 20 min. After 6 h, the reaction mixture was poured into non-solvent (methanol), filtered, washed several times with methanol, and dried in vacuum for 48 h. PAni.DBSA prepared by this procedure exhibited a surface conductivity of 2.1 S/cm.

### Blend preparation

#### Melt mixing method

Different amounts of STF copolymer was introduced into a Haake Rheocord 9000 internal mixer operating with a CAM rotor at 120°C and 60 rpm. After 2 min, PAni.DBSA powder was added and mixing was continued for 8 min. The blends were then quickly sheeted in a two-roll mill.

#### *In situ* polymerization method

STF dissolved in toluene, in a fixed concentration of 10 wt %, to avoid high viscous medium. Keeping the same STF concentration in toluene and the same DBSA : aniline : APS molar ratios of 1 : 1 : 1, different STF/PAni weight ratios were obtained with different amounts of PAni.DBSA. The reaction was carried out at 0°C. After the polymerization, the emulsion of STF/PAni.DBSA was precipitated in methanol. The dark green precipitate was filtered, washed with methanol several times, and finally vacuum dried for 48 h. The conversion was determined gravimetrically. The amount of the PAni.DBSA determined gravimetrically and it was used to calculate the proportion of PAni in the blends. The composite specimens were compression-molded at 160°C for 10 min.

## TECHNIQUES

### Volume resistivity

STF/PAni blends were pressed into disks with 38 mm diameter using 4.5-ton hydraulic press at 100°C for 3 min. The volume resistivity ($R_v$) was measured as per the ASTM D-257 specification. The equipment used to perform the volume resistivity measurements was composed by an electrometer Keithley 6517A and a home-made four-probe device with an average probe distance of $0.17 \pm 0.03$ cm.

### Wide angle X-ray scattering

The WAXS measurements were performed at the WAXS/SAXS beam line of the LNLS (Laboratório Nacional de Luz Sincroton–Campinas, Brazil; D11A-SAXS1# 5324/06; D11A-SAXS1–7086/08), by using monochromatic beam with wavelength of 1.7433 Å. The scattering intensity was recorded with a two-dimensional detector, using a sample-detector distance of 1641.5 mm. In the case of WAXS, 2θ

corrections were computed with the help of $Al_2O_3$ patterns. The samples were scanned in the 2θ range of 10–60° at intervals of 0.03 employing a curved position sensitive detector in the transmission mode.

These patterns were indexed using TREOR procedure. The intensity was corrected for Lorentz-polarization factors and also for instrumental broadening using Stokes deconvolution method. The microstructural parameters such as the crystal size (<*N*>) and lattice strain [*g* (%)] are determined by employing Fourier methods.[20,21] Different microcrystalline parameters were evaluated for STF/PAni composites from the X-ray profiles by three mathematical models, namely the exponential, lognormal, and reinhold distribution methods. The theory of the X-ray profile analysis to evaluate the crystalline parameters is reported in our previous communications.[22,23]

## RESULTS AND DISCUSSION

### Volume resistivity

The obtained volume resistivity of PAni.DBSA and its blends with STF is given in Table I. From the table, it was noticed that percolation threshold occurred at about 30% PAni for the blends prepared by *in situ* method, but significantly percolation threshold value was obtained at high PAni loaded system (around 40%) is observed for the blends prepared by melt mixing method as expected. The blend prepared by in situ polymerization resulted in lower percolation threshold, is due to the favorable morphology characterized by the formation of interconnected microtubules, which form the conducting pathway with lower amount of PAni. However, in case of melt mixing method, PAni particles are distributed in the form of agglomerates in STF insulator phase, resulted in higher resistivity value. This result clearly indicates that the better electrical performance for the blends prepared by the *in situ* polymerization as compared to melt mixing method.

**TABLE I**
**Volume Resistivity Data of STF/PAni Blends**

| Sample code | PAni content in STF (wt %) | Volume resistivity (Ω cm) |
|---|---|---|
| STF | 0.0 | $(3.1 \pm 0.9) \times 10^{12}$ |
| Melt mix blends | | |
| STPH1 | 15.0 | $(4.2 \pm 0.8) \times 10^{12}$ |
| STPH2 | 30.0 | $(4.08 \pm 0.07) \times 10^{7}$ |
| STPH3 | 45.0 | $(6.48 \pm 0.06) \times 10^{4}$ |
| *In situ* blends | | |
| STPIS1 | 22.3 | $(7.07 \pm 0.03) \times 10^{5}$ |
| STPIS2 | 27.0 | $(1.75 \pm 0.01) \times 10^{4}$ |
| STPIS3 | 51.5 | $(7.98 \pm 0.04) \times 10^{3}$ |
| PAni | 100 | – |

### X-ray diffraction

To probe the microstructure of conducting blends, the powder X-ray diffraction patterns of the STF, PAni, and STF/PAni blends were recorded. X-ray diffractograms recorded for PAni, STF, and both series of their blends are shown in Figure 1. In the case of PAni.DBSA diffractogram, several sharp reflections and STF diffractogram has two broad amorphous peaks were observed. The most important of them include those at 2θ = 20.21, 21.59, 26.66, 29.84, and 34.60°.

The peak centered at 2θ = 20.2° may be ascribed to periodicity parallel to the polymer chain, while the peak at 2θ = 26.6° may be due to the periodicity perpendicular to the polymer chain.[24] The peak at 2θ = 20.2° also represents the characteristic distance between the ring planes of benzene rings in adjacent chains or the close contact interchain distance.[25] The Bragg peak at 26.6° with lattice spacing (*d*) of 3.59 Å suggests that the dodecyl group of sodium dodecylsulfate (DBSA), which can act as a counter ion in the doping of the PAni.[26] The intense peak that appeared at around 2θ = 26.6° is a relatively sharp, well-defined peak, and the other peaks are also due to the Bragg-like order of the material associated with paracrystalline disorder.[27]

However, the interplanar distance of the main peak was found to be higher than the corresponding value of the less intense peaks and a slight variation with the composition of the blends. This implies that there is a change in the structure of the blends.

However, the diffractogram of the STF sample displayed a broad and intense peak at around 2θ = 22.09° and another small peak at around 2θ = 47.11°. The X-ray profiles of STF/PAni blends are significantly depends on the composition of the blends and synthetic routes. The blends also displayed multiple sharp reflections whose number and size depends upon the composition of PAni.DBSA in the blends and also the method used for blend preparation. Blends containing 15% of PAni.DBSA presented a diffractogram similar to that found in pure STF, indicating very low level of crystallinity. As the PAni.DBSA content in the blends increases, sharp peaks started to appear at 2θ = 28°, because of an increase on crystalline dispersed phase of PAni in amorphous STF matrix. The blends prepared via *in situ* polymerization showed less number of reflections, indicating lower degree of crystallinity and different molecular arrangements/crystal structures. In case of *in situ* polymerization blends, the system containing 51.5 wt % PAni showed the peak at 2θ = 28.6°, which reveals the presence of crystalline PAni. Furthermore, this result clearly indicates that the systems with lower content of PAni will not exhibit the crystalline peaks of PAni in the measured short

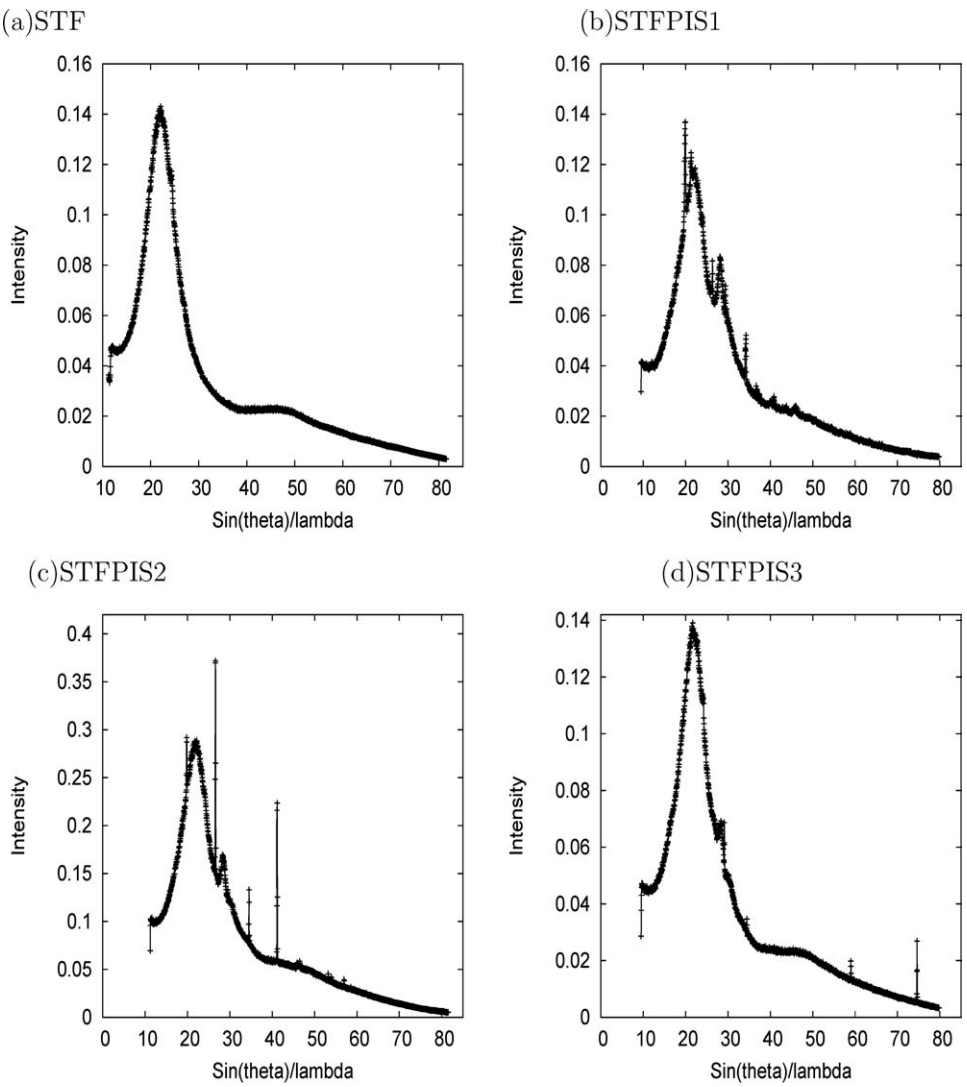


**Figure 1** WAXS patterns of (a) STF and melt mixed blends containing, (b) 22.3%, (c) 27%, and (d) 51.5% of PAni.DBSA.

range (between 70 and 100 Å). In case of melt mixed blends, three peaks was showed for system with lower PAni content (85/15 STF/PAni), whereas other blends with higher PAni content exhibited four peaks. This result indicates that the higher degree of crystallinity for melt mixed blends. This can be attributed to the self assembly of PAni molecules into aggregates. This phenomenon occurs in lower quantities in the case of *in situ* blends due to the higher degree of dispersion of PAni.DBSA.

The microcrystalline parameters such as the interplanar spacing ($d_{hkl}$), nanocrystal size ($<N>$), lattice strain [$g$ (%)], standard deviation (δ), surface weighted crystal size ($D_s$), and crystallite area for the PAni, STF, and STF/PAni blends were calculated using exponential, reinhold, and lognormal asymmetric distribution functions and the results are given in Tables II–IV, respectively. From Tables II–IV, it was noticed that the volume of the ordered regions increases with increasing PAni content. The volume of the ordered regions represents those regions in the polymer network, which contribute to the X-ray Bragg reflections. In real space, essentially, a lower number of columns participate in the Bragg like diffraction process. The increase in the intensity of the X-ray ($2\theta = 28^\circ$) with increasing PAni content can be attributed to the concentration of PAni, which have higher scattering factors.

The broadening of X-ray reflections observed in these STF/PAni.DBSA blends is attributed to microdefects,[22,23] which also contribute for the decreasing in crystal size ($<N>$) and increase in lattice strain or lattice disorder [$g$ (%)]. The number of unit cells (crystal size, $<N>$) counted in a direction perpendicular to the Bragg's plane is higher values for PAni and lower values for STF and their blends. Along with this, there is also a lattice disorder of second

**TABLE II**
**Microstructural Parameters of STF, PAni, and Their Blends from WAXS Data (Exponential Distribution Function)**

| Sample | Profile no. | 2θ (degree) | $D$ (Å) | $g$ (%) | $<N>$ | α | $D_s$ (Å) | Crystallite area in (Å)$^2$ | δ (%) |
|---|---|---|---|---|---|---|---|---|---|
| PAni | 1 | 20.21 | 2.523 | 0.6 | 74.02 | 3.48 | 186.8 ± 9.34 | 44234.0 | 0.05 |
| | 2 | 21.59 | 2.369 | 0.5 | 126.41 | 0.13 | 299.5 ±17.37 | | 0.06 |
| | 3 | 26.66 | 1.943 | 0.5 | 120.31 | 1.22 | 233.8 ± 9.35 | | 0.04 |
| | 4 | 29.84 | 1.752 | 0.5 | 165.8 | 0.10 | 290.5 ±26.15 | | 0.09 |
| | 5 | 34.60 | 1.535 | 0.1 | 154.3 | 0.07 | 236.8 ±18.94 | | 0.08 |
| STF | 1 | 22.09 | 4.550 | 0.1 | 2.81 | 1.15 | 12.8 ± 0.33 | 49.58 | 0.03 |
| | 2 | 47.11 | 2.181 | 0.6 | 1.78 | 1.79 | 3.9 ± 0.23 | | 0.06 |
| STPH1 | 1 | 21.90 | 4.590 | 0.1 | 4.74 | 100.00 | 21.8 ± 0.65 | 121.13 | 0.03 |
| | 2 | 28.20 | 3.580 | 0.1 | 4.25 | 0.50 | 15.2 ± 0.91 | | 0.06 |
| | 3 | 47.98 | 2.144 | 0.1 | 3.12 | 1.01 | 6.7 ± 0.33 | | 0.05 |
| STPH2 | 1 | 21.97 | 4.574 | 0.1 | 4.22 | 2.00 | 19.3 ± 0.34 | 129.09 | 0.02 |
| | 2 | 28.27 | 3.569 | 0.1 | 19.71 | 0.44 | 70.3 ± 6.33 | | 0.09 |
| | 3 | 30.03 | 3.364 | 0.1 | 4.40 | 0.67 | 14.8 ± 0.84 | | 0.06 |
| | 4 | 47.03 | 2.185 | 0.1 | 2.92 | 1.06 | 6.4 ± 0.32 | | 0.05 |
| STPH3 | 1 | 21.70 | 4.629 | 0.1 | 4.15 | 8.60 | 19.2 ± 0.58 | 145.57 | 0.03 |
| | 2 | 28.35 | 3.559 | 0.1 | 23.42 | 0.61 | 83.4 ± 6.67 | | 0.08 |
| | 3 | 30.07 | 3.360 | 0.1 | 4.53 | 0.46 | 15.2 ± 0.76 | | 0.05 |
| | 4 | 48.02 | 2.140 | 0.1 | 3.14 | 1.46 | 6.7 ± 0.26 | | 0.04 |
| STPIS1 | 1 | 21.62 | 4.647 | 0.1 | 2.25 | 2.03 | 10.5 ± 0.42 | 70.50 | 0.04 |
| | 2 | 46.75 | 2.197 | 0.1 | 3.07 | 1.62 | 6.7 ± 0.27 | | 0.04 |
| STPIS2 | 1 | 21.55 | 4.663 | 0.4 | 2.27 | 1.10 | 10.6 ± 0.32 | 71.69 | 0.03 |
| | 2 | 46.38 | 2.214 | 0.1 | 3.06 | 1.12 | 6.8 ± 0.27 | | 0.04 |
| STPIS3 | 1 | 22.19 | 4.529 | 0.1 | 5.05 | 5.24 | 22.9 ± 1.15 | 141.56 | 0.05 |
| | 2 | 28.61 | 3.528 | 0.1 | 2.56 | 0.86 | 9.0 ± 0.36 | | 0.04 |
| | 3 | 50.52 | 2.042 | 0.1 | 3.03 | 1.11 | 6.2 ± 0.25 | | 0.04 |

kind, known as paracrystallinity, and normally quantified as strain ($gd/d$), where "$d$" is the inter planar spacing.

To know the most suitable asymmetric distribution, fitness test was conducted using line profile simulation from the peak of the reflection to its

**TABLE III**
**Microstructural Parameters of STF, PAni, and Their Blends from WAXS Data (Reinhold Distribution Function)**

| Sample | Profile no. | 2θ (degree) | $d$ (Å) | $g$ (%) | $<N>$ | β | $D_s$ (Å) | Crystallite area in (Å)$^2$ | δ (%) |
|---|---|---|---|---|---|---|---|---|---|
| PAni | 1 | 20.21 | 2.523 | 0.5 | 73.81 | 9.30 | 186.2 ± 9.3 | 44725.0 | 0.05 |
| | 2 | 21.59 | 2.369 | 0.5 | 126.07 | 0.10 | 298.7 ± 20.9 | | 0.07 |
| | 3 | 26.66 | 1.943 | 0.5 | 120.26 | 1.36 | 233.7 ± 9.3 | | 0.04 |
| | 4 | 29.84 | 1.752 | 0.1 | 162.20 | 0.12 | 284.2 ± 22.7 | | 0.08 |
| | 5 | 34.60 | 1.535 | 0.4 | 156.51 | 6.13 | 240.2 ± 19.2 | | 0.08 |
| STF | 1 | 22.09 | 4.550 | 0.1 | 2.81 | 1.71 | 12.8 ± 0.3 | 48.5 | 0.03 |
| | 2 | 47.11 | 2.181 | 0.5 | 1.76 | 2.35 | 3.8 ± 0.3 | | 0.06 |
| STPH 1 | 1 | 21.90 | 4.590 | 0.1 | 4.74 | 100.00 | 21.8 ± 0.6 | 120.4 | 0.03 |
| | 2 | 28.20 | 3.580 | 0.1 | 4.18 | 0.73 | 15.0 ± 1.0 | | 0.07 |
| | 3 | 47.98 | 2.144 | 0.1 | 3.10 | 1.46 | 6.6 ± 0.3 | | 0.05 |
| STPH 2 | 1 | 21.97 | 4.574 | 0.1 | 4.22 | 2.94 | 19.3 ± 0.3 | 121.6 | 0.02 |
| | 2 | 28.27 | 3.569 | 0.1 | 19.72 | 0.61 | 70.4 ± 6.3 | | 0.09 |
| | 3 | 30.03 | 3.364 | 0.1 | 4.38 | 0.97 | 14.7 ± 0.8 | | 0.06 |
| | 4 | 47.03 | 2.185 | 0.1 | 2.89 | 1.51 | 6.3 ± 0.3 | | 0.05 |
| STPH 3 | 1 | 21.70 | 4.629 | 0.1 | 4.16 | 3.56 | 19.3 ± 0.6 | 129.3 | 0.03 |
| | 2 | 28.35 | 3.559 | 0.1 | 23.42 | 0.78 | 83.4 ± 6.7 | | 0.08 |
| | 3 | 30.07 | 3.360 | 0.1 | 4.38 | 0.65 | 14.7 ± 0.7 | | 0.05 |
| | 4 | 48.02 | 2.140 | 0.1 | 3.13 | 2.10 | 6.7 ± 0.3 | | 0.04 |
| STPIS 1 | 1 | 21.62 | 4.647 | 0.1 | 2.25 | 3.35 | 10.5 ± 0.4 | 70.4 | 0.04 |
| | 2 | 46.75 | 2.197 | 0.1 | 3.06 | 2.31 | 6.7 ± 0.3 | | 0.04 |
| STPIS 2 | 1 | 21.55 | 4.663 | 0.4 | 2.25 | 1.57 | 10.5 ± 0.3 | 71.4 | 0.03 |
| | 2 | 46.38 | 2.214 | 0.1 | 3.05 | 1.66 | 6.8 ± 0.3 | | 0.04 |
| STPIS 3 | 1 | 22.19 | 4.529 | 0.1 | 5.02 | 7.40 | 22.7 ± 1.1 | 140.8 | 0.05 |
| | 2 | 28.61 | 3.528 | 0.1 | 2.53 | 1.24 | 8.9 ± 0.4 | | 0.05 |
| | 3 | 50.52 | 2.042 | 0.1 | 3.03 | 1.62 | 6.2 ± 0.3 | | 0.05 |

**TABLE IV**
**Microstructural Parameters of STF, PAni, and Their Blends from WAXS Data (Lognormal Distribution Function)**

| Sample | Profile no. | 2θ (degree) | $d$ (Å) | $g$ (%) | $L$ (area) | $P$ (2) | $P$ (3) | $D_s$ (Å) | Crystallite area in (Å)$^2$ | δ |
|---|---|---|---|---|---|---|---|---|---|---|
| PAni | 1 | 20.21 | 2.523 | 0.5 | 66.1 | 99.1 | 0.0007 | 166.8 ± 15.0 | 25603.8 | 0.09 |
| | 2 | 21.59 | 2.369 | 0.6 | 100.0 | 170.5 | 0.0005 | 236.9 ± 23.6 | | 0.10 |
| | 3 | 26.66 | 1.943 | 0.6 | 100.0 | 161.1 | 0.0002 | 194.3 ± 21.4 | | 0.11 |
| | 4 | 29.84 | 1.752 | 0.1 | 100.0 | 102.6 | 0.6433 | 175.2 ± 15.8 | | 0.09 |
| | 5 | 34.60 | 1.535 | 0.1 | 100.0 | 132.6 | 0.5014 | 153.5 ± 15.3 | | 0.10 |
| STF | 1 | 22.09 | 4.550 | 0.2 | 2.63 | 3.94 | 0.0024 | 12.0 ± 0.48 | 44.4 | 0.04 |
| | 2 | 47.11 | 2.181 | 0.5 | 1.68 | 2.52 | 0.0364 | 3.7 ± 0.22 | | 0.06 |
| STPH 1 | 1 | 21.90 | 4.590 | 0.3 | 4.42 | 3.58 | 0.5558 | 20.3 ± 0.61 | 103.2 | 0.03 |
| | 2 | 28.20 | 3.580 | 0.1 | 4.26 | 6.39 | 0.0214 | 15.3 ± 1.22 | | 0.08 |
| | 3 | 47.98 | 2.144 | 0.1 | 2.92 | 4.37 | 0.0301 | 6.3 ± 0.38 | | 0.06 |
| STPH 2 | 1 | 21.97 | 4.574 | 0.1 | 3.77 | 5.65 | 0.0087 | 17.2 ± 0.51 | 107.3 | 0.03 |
| | 2 | 28.27 | 3.569 | 0.5 | 19.49 | 11.12 | 0.6950 | 69.6 ± 6.90 | | 0.10 |
| | 3 | 30.03 | 3.364 | 0.1 | 4.17 | 6.21 | 0.0557 | 14.0 ± 0.60 | | 0.06 |
| | 4 | 47.03 | 2.185 | 0.1 | 2.73 | 4.09 | 0.0067 | 6.0 ± 0.36 | | 0.06 |
| STPH 3 | 1 | 21.70 | 4.629 | 0.1 | 3.73 | 5.59 | 0.0198 | 17.3 ± 0.86 | 127.4 | 0.05 |
| | 2 | 28.35 | 3.559 | 0.1 | 22.58 | 14.13 | 0.6610 | 80.4 ± 6.43 | | 0.08 |
| | 3 | 30.07 | 3.360 | 0.1 | 4.46 | 6.68 | 0.0148 | 15.0 ± 1.05 | | 0.07 |
| | 4 | 48.02 | 2.140 | 0.1 | 2.88 | 4.31 | 0.0189 | 6.2 ± 0.25 | | 0.04 |
| STPIS 1 | 1 | 21.62 | 4.647 | 0.1 | 2.03 | 3.05 | 0.0049 | 9.4 ± 0.47 | 55.3 | 0.05 |
| | 2 | 46.75 | 2.197 | 0.1 | 2.79 | 4.18 | 0.0127 | 6.1 ± 0.24 | | 0.04 |
| STPIS 2 | 1 | 21.55 | 4.663 | 0.4 | 2.24 | 3.35 | 0.0396 | 10.5 ± 0.52 | 57.7 | 0.05 |
| | 2 | 46.38 | 2.214 | 0.1 | 2.38 | 4.24 | 0.0026 | 5.3 ± 0.25 | | 0.05 |
| STPIS 3 | 1 | 22.19 | 4.529 | 0.1 | 4.66 | 3.94 | 0.5357 | 21.1 ± 1.05 | 122.4 | 0.05 |
| | 2 | 28.61 | 3.528 | 0.1 | 2.53 | 3.80 | 0.0108 | 8.9 ± 0.53 | | 0.06 |
| | 3 | 50.52 | 2.042 | 0.1 | 2.83 | 4.24 | 0.0147 | 5.8 ± 0.29 | | 0.05 |

baseline. The experimental and simulated X-ray profiles for the PAni, STF, and STF/PAni blends calculated using all the distribution functions. For the sake of comparison, specimen profiles obtained from exponential distribution function for PAni (five peaks), STF (two peaks), and STF/PAni (melt mix) blend (four peaks; Fig. 2). It is evident from the figure that there is good agreement between the experimental and theoretically calculated X-ray profiles. In all cases, it was noticed that the goodness of the fit was <15%. It is evident from this figure that the experimental data and the model parameters based on exponential and Reinhold distribution functions are quite reliable. These methods for obtaining microstructure parameters were also reliable in other systems.[28] These results are further justified by the behavior of the microstructural quantities such as the crystal size or correlation length (<$N$>) and lattice strain ($g$) at the microscopic level (Tables II–IV).

The $D_s$ results clearly indicated that the degree of crystallinity present at the surface was depends on the concentration of PAni and the synthetic routes of the blends. The physical interpretation of the crystal imperfection parameters such as <$N$> and $g$ essentially indicated the deviation in the lattice ordering for a distance of $D = Nd_{hkl}$ (Å) along the direction normal to the Bragg (*hkl*) plane. The variation in the $D_s$ values of the blends is due to the change in the morphology of the STF after blends with PAni. The peak intensity, <$N$>, and $D_s$ values at 2θ = 28.2° increases with increase in PAni content in both series of blends. In lognormal method, crystalline parameters such as $L$ and $P$(2) are increased with increase in PAni content. The variation in microcrystalline behavior at 2θ = 28.2° clearly indicates that the presence PAni and its influence on the morphological behavior of the blends. From Tables II–IV, it was noticed that higher crystallite area for conducting PAni and lower values for amorphous STF copolymer. However, the values of crystallite area for the blends are lies between PAni and STF and their range is: 103–145 and 55.3–141.56 for melt mix and *in situ* blends, respectively. In each blends series, the variation of crystallite area also significantly depends on the composition of PAni. The increase in crystallite area with PAni content can be associated to cooperative movements of the molecular chains that form at the amorphous region and at the interfacial regions. Such movements trigger motions in the crystalline phase, which result in increase in crystallite area. This is in agreement with the observations made by earlier investigations for entirely different class of materials.[29,30]

Tables II–IV also reveals that the higher values of nanocrystal size, $D_s$ (at 2θ = 28.6°) and crystallite area values for melt mix blend as compared to *in*

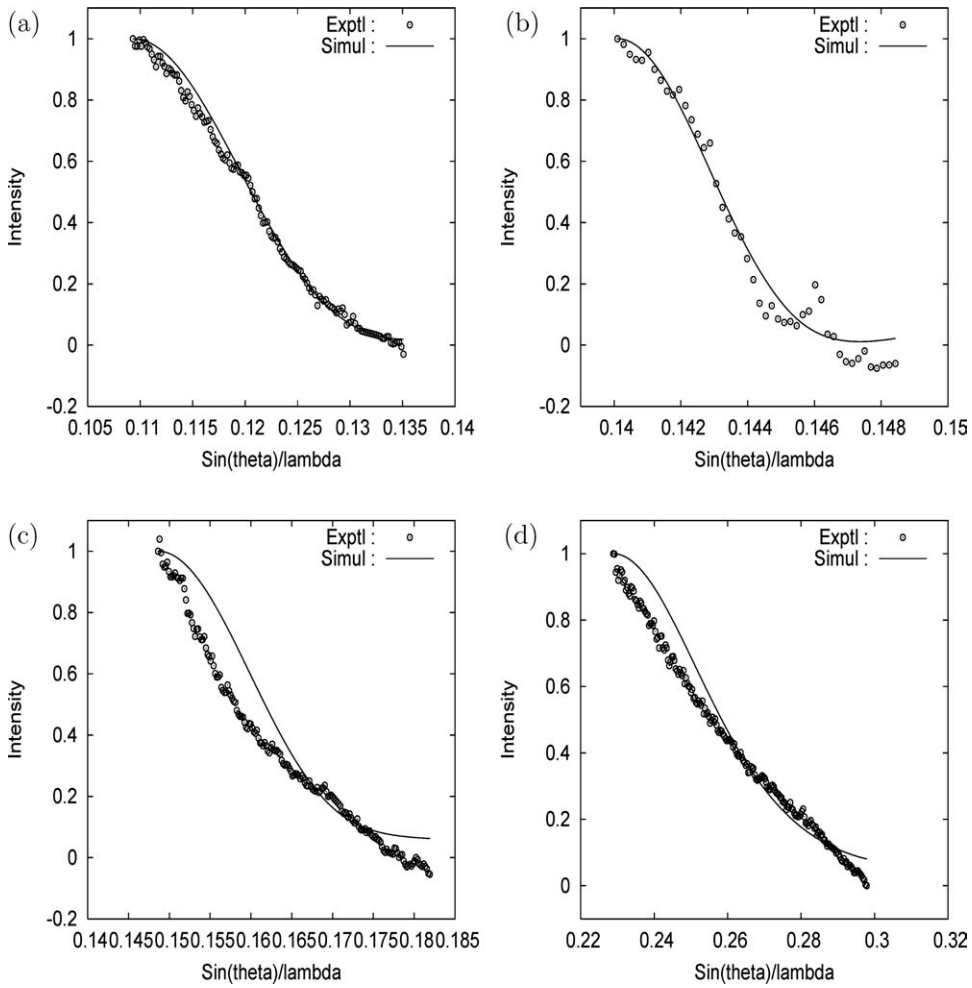


**Figure 2** Experimental and simulated X-ray profiles for melt mixed blend of STF with 30% PAni (STPH2) using Reinhold distribution function.

*situ* blends. This result indicates that the agglomerated PAni in STF matrix in melt mix methods causes for higher values of microcrystalline parameters. However, incase of *in situ* blends well-dispersed PAni exhibited poor microcrystalline behavior in the measured range. It was observed that the microcrystalline parameters calculated by using exponential and reinhold distribution functions give good agreement as compared to the results of lognormal distribution function.

From Tables II–IV, it is also evident that the exponential and reinhold distribution functions has a smaller standard deviation (δ) than the lognormal distribution function and, hence, we have preferred the corresponding results for further interpretation. The terms α and β are the width of the exponential distribution and the width of the reinhold distribution, respectively. These distributions are those of the crystallite size in the phase. The intensity of the scattered X-rays depends on the settings. It is the shape of the profile that is evaluated by the different models. If these are small implies a sharp distribution function in which case the system has a unique set of crystallites, and if it is large implies a wide distribution function, which essentially implies that the system has crystallites of various sizes and shapes. It is evident from Tables II and III that the width of the crystallite distribution will not follow any trend with the composition of the blends.

The computed microstructural parameters were used for computing the shape of the coherent domains in the form of ellipsoids using the surface weighted crystal size ($D_s$) values, corresponding to the average 2θ values along the $x$ and $y$ axes, respectively, and the same is shown in Figure 3. From this figure, it is evident that there are significant changes only at the periphery of the crystallite shape ellipsoid for the STF/PAni blends. It was also noticed that the crystallite size ellipse increases with increasing PAni content and higher crystallite size for the melt mix blends than *in situ* blends, as expected. According to Hosemann's model, these changes in the crystal size values as well as the shape ellipsoids

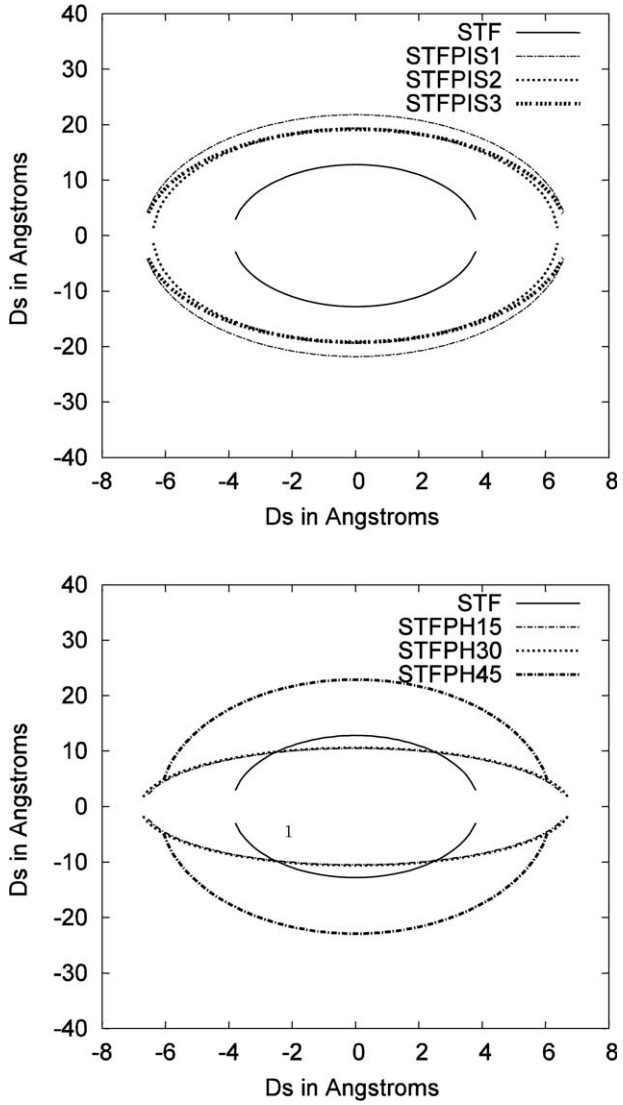


**Figure 3** The crystallite ellipsoid shape of the STF and STF/PAni.DBSA blends for (a) melt mixed and (b) *in situ* blends.

are attributed to the interplay between the strain present in the polymer network and the number of unit cells coherently contributing to the X-ray reflection.

From these tables, it was evident that the increase in crystallite size causes a decrease in volume resistivity, associated with slight reduction in lattice disorder measured in terms of the "*g*" parameter.

## CONCLUSIONS

To probe the effect of synthetic routes and PAni composition on the microstructural behavior of STF/PAni blends, WAXS pattern have been recorded. The X-ray results revealed that there is a significant increase in microcrystalline parameters such as nanocrystal size (<*N*>), crystallite area and $D_s$ (at 2θ = 28.2°) with increasing PAni content in the amorphous STF matrix, as expected. Among the synthetic methods, melt mixed blends exhibited higher values of <*N*>, $D_s$ and crystallite area as compared to *in situ* blends. This is due to the formation of physical interpenetrating network in case of *in situ* blends. Therefore, there was no formation of domains of aggregates by PAni chains in large extent due to the interconnection of STF chains. The absence of large range aggregates reduces the degree of crystallinity level but promotes conducting network formation at lower PAni content. However, incase of melt mix blends agglomeration of PAni crystallites takes place in amorphous STF matrix, which causes for higher degree of crystalline behavior. This result clearly indicates that the microcrystalline behavior of the blends depends on the methods of synthetic routes (morphology) and composition (PAni content) of the blends. The increase in crystallite size with increase in PAni supports the electrical behavior of the blends.

The authors would like to thank Laboratório Nacional de Luz Sincontron for the technical support on the WAXS experiments.

## References

1. Chen, S. A.; Fang, Y. Synth Met 1993, 60, 215.
2. Ziemells, K. Nature 1998, 393, 619.
3. Martins, C. R.; Freitas, P. S.; Paoli, M. A. Polym Bull 2003, 49, 379.
4. Ameena, S.; Ali, V.; Zulfequar, M.; Mazharul Haq, M.; Husain, M. Phys B: Condens Matter 2008, 403, 2861.
5. Yang, X.; Zhao, T.; Yu, Y.; Wei, Y. Synth Met 2004, 142, 57.
6. Jeevananda, T.; Palaniappan, S.; Siddaramaiah. J Polym Mater 2000, 17, 313.
7. Chipara, M.; Hui, D.; Notingher, P. V.; Chipara, M. D.; Lau, K. T.; Sankar, J. Comp Part B: Eng 2003, 34, 637.
8. Gamgopadhyay, R.; De, A.; Ghosh, G. Synth Met 2001, 123, 21.
9. Mirmohseni, A.; Wallace, G. G. J Polym 2003, 44, 3523.
10. Thanpitcha, T.; Sirivat, A.; Jamieson, A. M.; Rujiravanit, R. Carbohydr Polym 2006, 64, 560.
11. Vicentini, D. S.; Guilherme, M. O.; Barra, J. R.; Bertolino.; Pires, A. T. N. Eur Polym J 2007, 43, 4565.
12. Park, Y.; Chol, S.; Song, S.; Miyata, S. J Appl Polym Sci 1992, 46, 843.
13. Ebrahim Sh.; Kashyout, A.; Soliman, M. J Polym Res 2007, 14, 23.
14. Fernando G. S., Jr.; Bluma G. S.; Siddaramaiah; Guilherme, M. O.; Barra; Herbst, M. H. Polymer 2006, 47, 7548.
15. Jeevananda, T.; Siddaramaiah. Polym Eng Sci 2003, 43, 1138.
16. Jeevananda, T.; Siddaramaiah; Seetharamu, S.; Saravanan; D'Souza, L. Synth Met 2004, 140, 247.
17. Jeevananda, T.; Siddaramaiah; Joong-Hee, L.; Samir, O. M.; Somashekar, R. J Appl Polym Sci 2008, 109, 200.
18. Fernando G. S., Jr.; Bluma G. S.; Mantovanl, G. L.; Manjunath, A.; Somashekarappa, H.; Somashekar, R.; Siddaramaiah. Polymer 2006, 47, 2163.
19. Knoll, K.; Niebner, N. Macromol Symp 1998, 132, 231.
20. Warren, B. E. Acta Crystallogr 1955, 8, 483.

21. Warren, B. E. X-ray Diffraction; Addison-Wesley: New York, 1969.
22. Kumar, H.; Siddaramaiah; Somashekar, R.; Mahesh, S. S. Mater Sci Eng A 2007, 447, 58.
23. Somashekar, R.; Somashekarappa, H. J Appl Cryst 1997, 30, 147.
24. Moon, Y. B.; Cao, Y.; Smith, P.; Heeger, A. J Polym Commun 1989, 30, 196.
25. Pouget, J. P.; Hsu, C. H.; MacDiarmid, A. G.; Epstein, A. J Synth Met 1995, 69, 119.
26. Pouget, J. P.; Jozefowicz, M. E.; Epstein, A. J.; Tang, X.; MacDiarmid, A. G. Macromolecules 1991, 24, 779.
27. Chaudhari, H. K.; Kelkar, D. S. Polym Int 1997, 42, 380.
28. Jeevananda, T.; Siddaramaiah; Annadurai, V.; Somashekar, R. J Appl Polym Sci 2001, 82, 383.
29. Kumar, H.; Siddaramaiah.; Somashekar, R.; Mahesh, S. S.; Abhishek, S.; Guru Row, T. N.; Kini, G. S. J Appl Polym Sci 2006, 99, 177.
30. Popa, N. C.; Balzar, D. J Appl Cryst 2002, 35, 338.